

A CFD Analysis of Hydraulic Characteristics of the Rod Bundles in the BREST-OD-300 Wire-Spaced Fuel Assemblies

Dmitry V. Fomichev, Vladimir I. Solonin

Open Science Index, Physical and Mathematical Sciences Vol:8, No:7, 2014 publications.waset.org/9989996.pdf

Abstract—This paper presents the findings from a numerical simulation of the flow in 37-rod fuel assembly models spaced by a double-wire trapezoidal wrapping as applied to the BREST-OD-300 experimental nuclear reactor. Data on a high static pressure distribution within the models, and equations for determining the fuel bundle flow friction factors have been obtained. Recommendations are provided on using the closing turbulence models available in the ANSYS Fluent. A comparative analysis has been performed against the existing empirical equations for determining the flow friction factors. The calculated and experimental data fit has been shown.

An analysis into the experimental data and results of the numerical simulation of the BREST-OD-300 fuel rod assembly hydrodynamic performance are presented.

Keywords—BREST-OD-300, wire-spaces, fuel assembly, computation fluid dynamics.

I. INTRODUCTION

THE core of the BREST-OD-300 lead-cooled experimental nuclear reactor [1], [2] uses two types of fuel assemblies (FA): the central zone (CZ) assemblies and the peripheral zone (PZ) assemblies. The only structural difference between said fuel assemblies are the diameters of the fuel rods spaced inside a regular triangular lattice.

One of the fuel element spacing options is a double-wire trapezoidal wrapping (a ‘rib-on-rib’ spacing type). For the CZ FAs and the PZ FAs respectively, the relative fuel element pitch (S/d) is 1.33 and 1.23, and the relative wrapping pitch (T/d) is 20.6 and 19.

Out of a great deal of theoretical and experimental data on hydrodynamics of fuel rod bundles (both bare and wrapped) [3]-[6], there is only a limited number of those meeting the requirement for the proximity of the major geometrical characteristics (in terms of spacing method, relative fuel element pitch (S/d), and relative wrapping pitch (T/d)), required for the BREST-OD-300 fuel assemblies.

A topical task is therefore to acquire new experimental data and generalize the numerical simulation analysis of the flow in the fuel rod bundles spaced by a double-wire trapezoidal wrapping so that to define more accurately their hydraulic characteristics.

D. V. Fomichev is with the JSC “N.A. Dollezhal R&D Institute of Power Engineering” (JRS “NIKIET”), Moscow, Russia (phone: +7-926-279-0444; e-mail: fomichev@nikiet.ru; dmifomichev@gmail.com).

V. I. Solonin is with the Bauman Moscow State Technical University, Moscow, Russia (e-mail: en7@power.bmstu.ru).

II. EXPERIMENTAL MODELS AND RESULTS

The 37-rod models of the CZ and PZ assemblies have been made at the Bauman Moscow State Technical University (BMSTU). The model rod diameters have been scaled at $\sim 2:1$. The rod bundle length is 1040 mm. The rod bundle is enclosed within a hexagonal housing with the inside width across flats of 173 mm. The rods are spaced by a double-wire trapezoidal wrapping of the ‘rib-on-rib’ type.

Table I gives the major geometrical characteristics of the CZ and PZ FAs.

TABLE I
 GEOMETRICAL CHARACTERISTICS OF THE CZ AND PZ FA MODELS

Symbol	Quantity	Value for	
		CZ FA	PZ FA
d (mm)	fuel rod simulator outer diameter	20.81	22.53
h_1 (mm)	trapezoidal wrapping lower base	4.29	3.65
h_2 (mm)	trapezoidal wrapping upper base	2.15	
h_0 (mm)	trapezoidal wrapping height	3.38	2.52
D (mm)	fuel rod simulator width across corners	27.47	
S (mm)	fuel rod simulator pitch	27.57	
T (mm)	spacer wire pitch	429	
δ_1 (mm)	biggest gap between two adjoining spacer wires	0.1	
δ_2 (mm)	biggest gap between housing and spacer wires	1.0	
L (mm)	fuel rod simulator length	1040	
S/d	relative fuel rod simulator pitch	1.33	1.23
T/d	relative trapezoidal wrapping pitch	20.6	19.0
$d_{c,ex}$	hydraulic diameter (rod bundle flow passage, excluding housing)	17.37	13.84
$d_{c,in}$	hydraulic diameter (rod bundle flow passage, including housing)	14.34	12.28

The experiments included measurements of the static pressure (p) distribution along two housing facets on the generators between two adjoining peripheral rods using pressure take-offs and the data measuring system of BMSTU’s Nuclear Reactors and Plants Department. With a given flow rate, 19 pressure values were measured along the model height (z).

The results of the experiments have been generalized by the following equations to determine the flow friction factors:

- CZ FA model:

$$\lambda = 0.311 \times \text{Re}^{-0.244}, \Delta = 6\% . \quad (1)$$

- PZ FA model:

$$\lambda = 0.154 \times \text{Re}^{-0.153}, \Delta = 5\% . \quad (2)$$

The flow friction factor (λ) has been obtained from the relation [8].

$$\frac{1}{\lambda} \frac{dp}{dz} = \frac{1}{d_{c,in}} \frac{\rho w^2}{2}, \quad (3)$$

where w is the mass-averaged flow rate in the rod bundle flow passage, m/s ; ρ is the average flow density, kg/m^3 ; and $d_{c,in}$ is the model's hydraulic diameter, m .

The Reynolds number is determined from the hydraulic diameter of the rod bundle flow passage (without the model's housing taken into account) using the following equation [8]

$$Re = \frac{w d_{c,ex}}{\nu}, \quad (4)$$

where ν is the kinematic viscosity, m^2/s .

The application interval for the equations obtained lies in the range of Reynolds numbers $(3.5 \dots 6.5) \times 10^4$. The errors Δ take into account deviations of the flow parameters and the model geometry.

For the two experimental flow modes in the CZ and PZ FA models, a numerical simulation has been performed using the ANSYS Fluent 14.5 [8].

The FA model geometrical and computational models used for numerical calculations are given in Fig. 1.

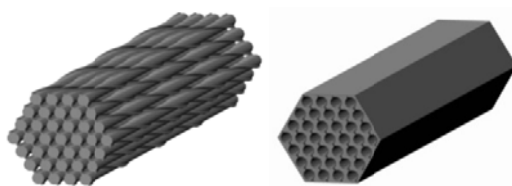


Fig. 1 FA model geometrical (a) and computational (b) models

III. MESH AND BOUNDARY CONDITIONS

The computational mesh for the CZ and PZ FA models was constructed in two steps. At step 1, a tetrahedral computational mesh was built using the ANSYS Meshing [9]. At step 2, the tetrahedral mesh was adapted and converted to a polyhedral mesh using the ANSYS computational mesh operation functions. The total number of the computational mesh elements was $\sim 10^8$. Fragments of the computational mesh for the CZ FA model are shown in Fig. 2.

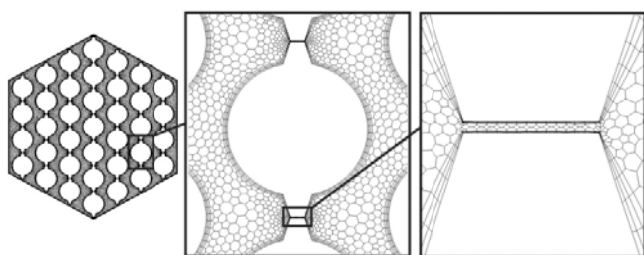


Fig. 2 Fragments of the CZ FA model computational mesh

The FA model computational model includes the following boundary conditions: uniform flow rate distribution at the model's inlet and stability of the flow static pressure at the FA model outlet. The fluid is air the properties of which are defined by the ideal gas law.

IV. TURBULENCE MODELS

For the rod bundle flow analyses, 7 turbulence models available in the ANSYS Fluent [8] were considered, including the following models: Standard k- ϵ , Realizable k- ϵ , RNG k- ϵ , Standard k- ω , SST k- ω , SA and RSM. These models have been selected for the following reasons.

The Standard k- ϵ model [10] uses two differential transfer equations for the kinetic turbulence energy k and for the kinetic turbulence energy dissipation rate ϵ , as obtained from the Navier-Stokes and Reynolds equations using a given number of assumptions and hypotheses [10], [11].

The transfer equations, with no regard for the effects of buoyancy and extra turbulence generation and dissipation production sources, are written as follows

$$\frac{\partial \rho k}{\partial t} + \frac{\partial}{\partial x_i} (\rho k u_i) = \frac{\partial}{\partial x_j} \left[\left(\mu + \frac{\mu_t}{\sigma_k} \right) \frac{\partial k}{\partial x_j} \right] + G_k - \rho \epsilon - Y_k, \quad (5)$$

$$\frac{\partial \rho \epsilon}{\partial t} + \frac{\partial}{\partial x_i} (\rho \epsilon u_i) = \frac{\partial}{\partial x_j} \left[\left(\mu + \frac{\mu_t}{\sigma_k} \right) \frac{\partial \epsilon}{\partial x_j} \right] + C_{1\epsilon} \frac{\epsilon}{k} G_k - C_{2\epsilon} \rho \frac{\epsilon^2}{k}, \quad (6)$$

where $G_k = \rho \overline{u_i' u_j'} \frac{\partial u_j}{\partial x_i}$ is the turbulent kinetic energy generation; $Y_k = 2 \rho \epsilon M_t^2$ is the factor allowing for the conditions of the air current flow compressibility as the ideal gas; $M_t = \sqrt{\frac{k}{a^2}}$ is the turbulent Mach number; $a = \sqrt{\gamma R T}$ is the velocity of the sound in the air current.

The turbulent dynamic viscosity is determined from the following relation

$$\mu_t = \rho C_\mu \frac{k^2}{\epsilon}. \quad (7)$$

A standard set of constants has been formed for this model:

$$C_{1\epsilon} = 1.44, C_{2\epsilon} = 1.92, C_\mu = 0.09, \sigma_k = 1.0, \sigma_\epsilon = 1.3.$$

The Standard k- ϵ turbulence model allows applied flows with a moderate deformation of the velocity fields to be calculated.

For flows with a heavily curved current line, the RNG k- ϵ model is recommended in which the structure of the transfer equations for the turbulence kinetic energy and dissipation rate are the same as for the Standard k- ϵ model, but a special differential equation is used to determine the turbulence viscosity [12].

The experience of using this model shows a better (as compared against the Standard k-ε model) fit of the calculated and experimental data, specifically for the flows with a heavily curved current line.

The Realizable k-ε model [13] is also recommended for flows with the current lines heavily curved and the flow heavily swirled. The model uses a mean vortex motion transfer equation and eliminates the negative values for the quantity $\overline{u_j^2}$ when the average rate distributions are heavily deformed. The model's parameter C_μ depends on the flow characteristics.

The Reynolds stress model (RSM) [14], [15] does not use the turbulent viscosity hypothesis. Instead, differential transfer equations are solved for each Reynolds stress tensor component and the transfer equation is solved for the turbulence kinetic energy dissipation rate ϵ . This basically makes it possible to take into account the anisotropy of turbulent pulsation which extends considerably the model's application region, including for flows with the current lines heavily curved and the flow swirled. The drawback of the model is the approximate simulation of multiple correlations arising when the transfer equations are derived.

The Spalart-Allmaras (SA) model [16] contains one differential transfer equation for the modified kinetic turbulent viscosity $\tilde{\nu}$ related to the 'internal' turbulent viscosity $\nu_t = \mu_t / \rho$ through algebraic equations that contain the parameter $\tilde{\nu} / \nu$, where ν is the kinematic viscosity, and a number of constants [7].

For ϵ , instead of the transfer equation, the Standard k- ω model [17] uses the vortex motion equation $\omega = \epsilon / k$, which leads in a number of problems to a better fit with the experimental data than the Standard k-ε model.

The SST k- ω Menter model [18], [19] is a combination of Standard k-ε models and k- ω models. These models are merged through the empiric function F_1 , which ensures that the integrated model is close to the k-ε model away from solid walls and to the k- ω model in the near-wall flow. The turbulence viscosity determination uses the Bradshaw hypothesis [20] on the proportionality of the shear stress in the near-wall portion of the turbulent pulsation energy boundary layer, which helps avoid the separation delay representative of the k-ε models.

When the mesh in the near-wall calculation region is not detailed enough, a Standard near-wall function [21] was used for each of the presented models.

V. RESULTS

The results of the static pressure experimental determination and the calculated static pressure values obtained using different turbulence models for the flows in the CZ and PZ FA models, are presented in Figs. 3 and 4 respectively.

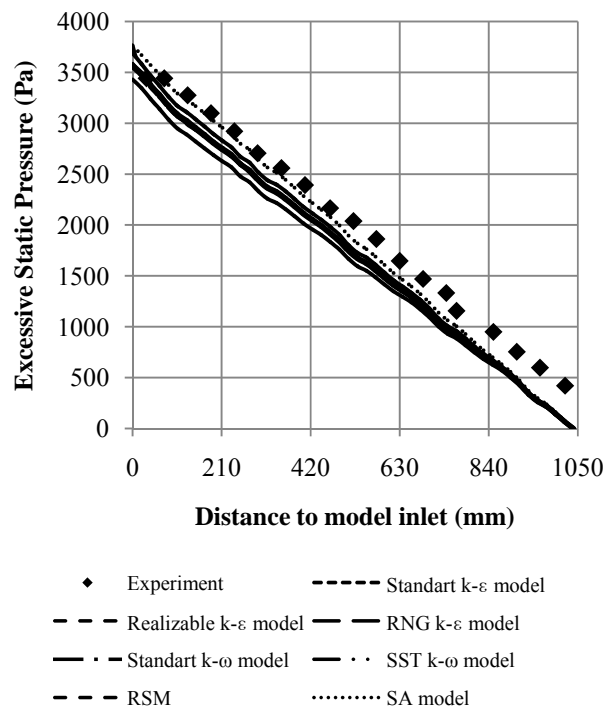


Fig. 3 Axial static pressure distribution in the CZ FA model

A comparison of the numerical flow simulation results for the CZ FA model against the experimental data shows that the static pressure is higher at the bundle outlet than that assumed in the calculation, which stems from the effects of the outlet spacer grid not having been taken into account. Therefore, the calculation and experiment fit was analyzed based on the static pressure gradient values as given in Table II.

TABLE II
AVERAGE STATIC PRESSURE GRADIENT VALUES FOR THE CZ FA MODEL

Parameter	Experiment	k-ε Standard	RNG k-ε	k-ε Realizable	k-ω Standard	k-ω SST	RSM	SA
Average Static Pressure Gradient, (Pa/m)	3.225	3.326	3.194	3.342	3.343	3.329	3.344	3.556
Flow friction factor	0.02949	0.03041	0.02921	0.03056	0.03139	0.03044	0.03058	0.03252

All turbulence models have been shown to fit the experimental data well enough, excluding the SA model. For the Standard k-ε model, and for the RNG k-ε and SST k-ω models, the calculation accuracy does not exceed 3%. The

accuracy was 3.5% in the event of the Realizable k-ε and RSM models, and 6% in the event of the Standard k-ω model. The worst variant was obtained with the use of the SA model intended primarily for the external flow problems.

A comparison of the numerical simulation results for the

flow in the PZ FA model against the experimental data (Fig. 4) shows the static pressure at the rod bundle outlet is a bit higher than the experimental pressure. The latter has been caused by the pressure recovery in the stream flow beyond the outlet spacer grid. The experimental static pressures in the rod bundle outlet region may be caused by a deviation of the rib geometry from the nominal geometry.

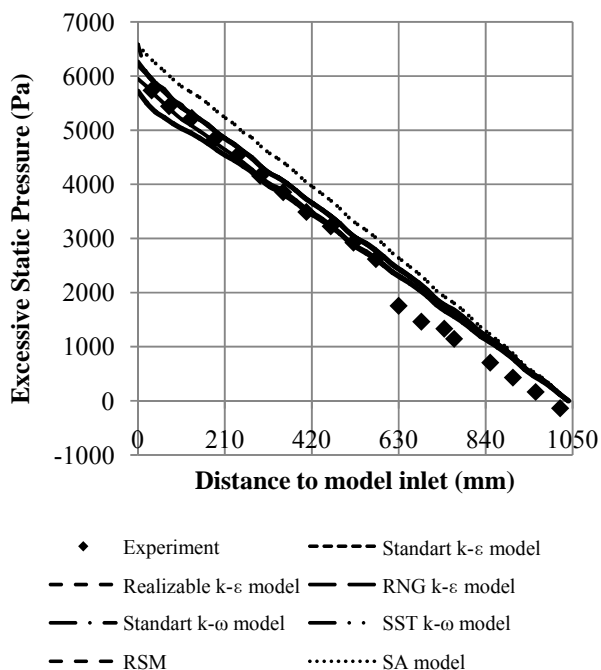


Fig. 4 Axial static pressure distribution in the PZ FA model

Table III presents a comparison of the static pressure gradients for the PZ FA model. The experimental gradient values have been defined using the initial 11 experimental points.

The SST $k-\omega$ model yields the best results. The accuracies of results obtained using the $k-\epsilon$ Standard, RNG $k-\epsilon$,

TABLE III
 AVERAGE STATIC PRESSURE GRADIENT VALUES FOR THE PZ FA MODEL

Parameter	Experiment	$k-\epsilon$ Standard	RNG $k-\epsilon$	$k-\epsilon$ Realizable	$k-\omega$ Standard	$k-\omega$ SST	RSM	SA
Average Static Pressure Gradient, (Pa/m)	5.7822	5.873	5.601	5.392	5.848	5.842	5.873	6.246
Flow friction factor	0.02767	0.0281	0.0268	0.0258	0.02798	0.02795	0.0281	0.02989

Generalizations of the MSTU-produced experimental data have been compared against the available research data on flow friction in the rod bundles spaced by helical ribs. It should be noted that [22], [23] do not contain geometrical characteristics of bundles. In experiments [24]-[26], the parameter values are $S/d < 1.3$ and $T/d \sim 8$. In experiments [27], the rods are spaced by a single-wire wrapping of the ‘ribbon-cladding’ type. In experiments [28], the rod number ranges from 19 to 217, and the parameters S/d and T/d are in the required intervals, but there is no data on the shape and number of the spacer ribs, likewise on the selection of the

Realizable $k-\epsilon$ and RSM models do not exceed 5%. The $k-\omega$ and SA models yield the biggest deviations from the experimental data.

Therefore, the Standard $k-\epsilon$ model, the RNG $k-\epsilon$ model or the SST $k-\omega$ model may be recommended for calculating the hydraulic loss in the BREST-OD-300 CZ and PZ fuel rod bundles. The use of the Standard $k-\epsilon$ model yields the calculation accuracy within a range of 3% as compared against MSTU’s experiments.

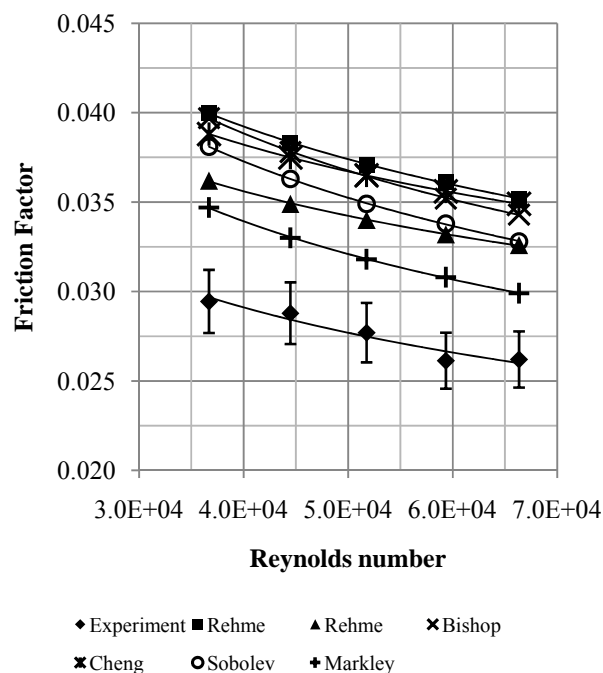


Fig. 5 Values of the flow friction factors for the CZ FA model test conditions

determining geometrical parameters for the flow friction factors and the Reynolds number.

A comparison against equations [22]-[28] is shown in Figs. 5 and 6 for the test conditions of the CZ and PZ FA models respectively.

For the CZ FA model, an acceptable fit with the experiments is provided by the Markley model [26] and the Rehme model [27]: 14 and 19% respectively (given that the accuracy of empirical equations is in the limits of 30%). Besides, it should be also taken into account that the Sobolev model [24] (aka the FEI formula recommended for the

calculation in the Technical Guides [25]) gives a conservative friction factor value of about 28%.

flow in rod bundles of the geometry considered for the BREST-OD-300 core FAs.

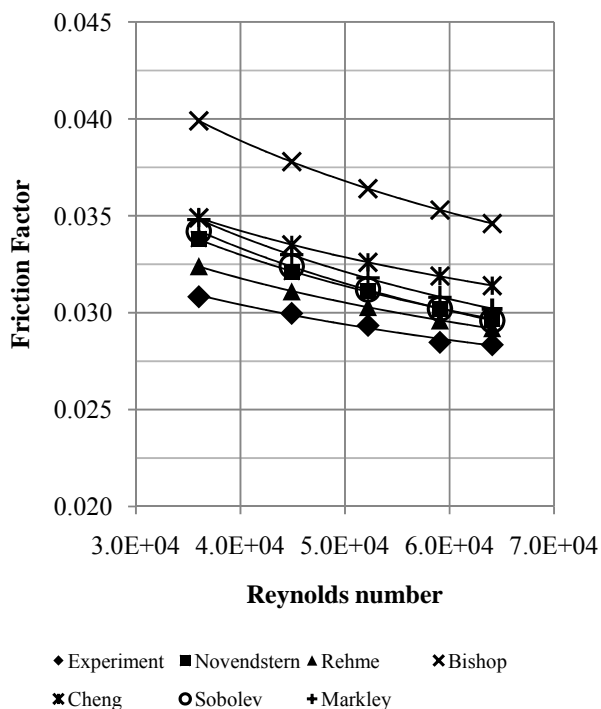


Fig. 6 Values of the flow friction factors for the PZ FA model test conditions

In the event of the PZ FA model, a fairly good fit (in the limits of 11%) is observed for all equations that have been considered, excluding the Bishop model [22].

VI. CONCLUSION

The experimentally obtained equations of flow friction factors (1) and (2) in 37-rod models of the BREST-OD-300 core CZ and PZ FAs for the central zone geometry conditions are close to the flow conditions in a smooth tube (the Blasius formula $\lambda = 0.3164 \times Re^{-0.25}$ [7]), and are close to the Cheng and Todreas equations [23] ($\lambda = C_f \times Re^{-0.18}$) for the conditions of the peripheral zone geometry. A conclusion may be made that an increase in the rib height leads to a decrease in the rib eddying effects on the rod bundle hydraulic loss, and the flow develops in the same way as in an equivalent round smooth tube. On the contrary, a shorter rib height gives an increased role to the rib eddying effects of the self-similar local loss type, with the equation on the Reynolds number being weakened.

The numerical simulation results, which fit well the experimental data obtained, show that there are periodic components in the static pressure variation in the quasi-steady flow resulting from flow swirling by the spacer ribs.

The Standard $k-\epsilon$ model, and the RNG $k-\epsilon$ and SST $k-\omega$ models may be recommended for the numerical simulation of

REFERENCES

- [1] *The White Book of Nuclear Energy* / V.V. Orlov, M.M. Seliverstov, V.A. Tishchenko, V.V. Uzhanova, V.S. Smirnov, I.Kh. Ganev, A.V. Lopatkin, S.V. Bryunin, A.N. Karhov, S.V. Yevropin, G.Ye. Shatalov, V.Ye. Sitnikov, P.I. Dolgosheev V.B. Kozlov, V.P. Fotin; ed. By Ye.O. Adamov. - M.: NIKIET Publishers, 1998. - 356 p. (in Russian).
- [2] Yu.G. Dragunov. *Technical Solutions and Development Phases of the BREST-OD-300 Reactor Facility* / Yu.G. Dragunov, V.V. Lemekhov, V.S. Smirnov, N.G. Chernetsov // J. Atomnaya Energiya.- 2012.- V. 113. No. 1. P. 58-64. (in Russian).
- [3] A.V. Sheynina. *Hydraulic Resistance of Rod Bundles in an Axial Fluid Flow* / A.V. Sheynina // Liquid Metals: collected works.- M.: Atomizdat, 1967. P. 210-223. (in Russian).
- [4] A.V. Zhukov. *An Analysis into the Hydraulic Resistance in Fuel Bundles of Fast-Neutron Reactors* / A.V. Zhukov, A.P. Sorokin, P.A. Titov, P.A. Ushakov // J. Atomnaya Energiya.- 1986. V. 60. No. 5. P. 317-321. (in Russian).
- [5] Bubelis, E. *Review and Proposal for Best-fit of Wire-wrapped Fuel Bundle Friction Factor and Pressure Drop Predictions Using Various Existing Correlations* / E. Bubelis, M. Schikorr.- Forschungszentrum Karlsruhe GmbH.- Karlsruhe, 2008.- 61 p.
- [6] *Turbulent Flow and Heat Transfer in Channels of Power Plants* / B.V. Dzyubenko, A. Sakalauskas, L. Ashmantas, M.D. Segal. - Vilnius: Pradai, 1995. - 300 p. (in Russian).
- [7] *Reference Book on Thermohydraulic Calculations in Nuclear Power. Thermohydraulic Processes in NPPs* / P.L. Kirillov, V.P. Bobkov, A.V. Zhukov, Yu.S. Yuryev; ed. by P.L. Kirillov.- M.: Izdat, 2010.- 776 p. (in Russian).
- [8] *ANSYS FLUENT, Theory Guide*, Rel. 14.5.- ANSYS Inc., 2012.
- [9] *ANSYS Meshing User's Guide*, Rel. 14.5.- ANSYS Inc., 2012.
- [10] Launder, B. E. *Lectures in Mathematical Models of Turbulence* / B. E. Launder, D. B. Spalding.- London, England: Academic Press, 1972.
- [11] A.Yu. Snegiryov. *High-Performance Computing in Engineering Physics. Numerical Simulation of Turbulent Flows: a textbook* / A.Yu. Snegiryov.- SPb.: Polytechnic University Publishing House, 2009.- 143 p. (in Russian).
- [12] Orszag, S. A. *Renormalization Group Modeling and Turbulence Simulations* / S.A. Orszag, V. Yakhot, W.S. Flannery, F. Boysan, D. Choudhury, J. Maruzewski, B. Patel // International Conference on Near-Wall Turbulent Flows / Tempe, Arizona, 1993.
- [13] Shih, T.-H. *A New Eddy-Viscosity Model for High Reynolds Number Turbulent Flows - Model Development and Validation* / T.-H. Shih, W.W. Liou, A. Shabbir, Z. Yang, and J. Zhu // Computers Fluids. 1995. No. 24 (3). P. 227-238.
- [14] Gibson, M.M. *Ground Effects on Pressure Fluctuations in the Atmospheric Boundary Layer* / M. M. Gibson, B. E. Launder. // J. Fluid Mech. 1978. No. 86. P. 491-511.
- [15] Launder, E. *Progress in the Development of a Reynolds-Stress Turbulence Closure* / E. Launder, G.J. Reece, W. Rodi // J. Fluid Mech. 1975. No. 68 (3). P. 537-566.
- [16] Spalart, P. *A One-Equation Turbulence Model for Aerodynamic Flows* / P. Spalart, S. Allmaras // American Institute of Aeronautics and Astronautics.- Technical Report AIAA-92-0439.- 1992.
- [17] Wilcox, D.C. *Turbulence Modeling for CFD* / D.C. Wilcox.- DCW Industries, Inc. La Canada, California, 1998.- 460 p.
- [18] Menter, F.R. *Two-Equation Eddy-Viscosity Turbulence Models for Engineering Applications* / F.R. Menter // AIAA Journal. 1994, No. 32 (8).- pp. 1598-1605.
- [19] Menter, F.R. *Ten Years of Experience with the SST Turbulence Model* / F. R. Menter, M. Kuntz, R. Langtry // Turbulence, Heat and Mass Transfer. 2003, No. 4. P. 625-632.
- [20] Bradshaw, P. *Calculation of Boundary Layer Development Using the Turbulent Energy Equation* / P. Bradshaw, D.H. Ferriss, N.P. Atwell // J. Fluid Mech. 1967. No. 28. P. 593-616.
- [21] Launder, B.E. *The Numerical Computation of Turbulent Flows* / B.E. Launder, D.B. Spalding // Computer Methods in Applied Mechanics and Engineering. 1974. No. 3. P. 269-289.
- [22] Bishop, A. *Hydraulic Characteristics of Wire-Wrapped Rod Bundles* / A. Bishop, N. Todreas // Nuclear Engineering and Design. 1980. No. 62 (1-3). P. 271-293.

- [23] Cheng, S.K. *Hydrodynamic Models and Correlations for Bare and Wire-Wrapped Hexagonal Rod Bundles - Bundle Friction Factors, Sub-channel Friction Factors and Mixing Parameters* / S.K. Cheng, N.E. Todreas // Nuclear Engineering and Design. 1986. No. 92. pp. 227-251.
- [24] Sobolev, V. *Fuel Rod and Assembly Proposal for XT-ADS Pre-design* / V. Sobolev // Coordination meeting of WP1&WP2 of DMI IP EUROTRANS / Bologna, 8-9 February, 2006.
- [25] *Guidelines, Rules, Methods of Calculation of Hydrodynamic and Thermal Characteristics of the Components and Equipment of Power Plants. Steering Technical Material: in 3 vols.* / Obninsk, 1991. - V. 1. - 435 p. (in Russian).
- [26] Engel, F. C. *Laminar, Transition and Turbulent Parallel Flow Pressure Drop across Wire-Wrap-Spaced Rod Bundles* / F.C. Engel, et al // Nuclear Science and Engineering. 1979. V. 69, pp. 290-296.
- [27] Rehme, K. *Pressure Drop Correlations for Fuel Element Spacers* / K. Rehme // Nuclear Technology. 1973. V. 17. pp. 15-23.
- [28] Novendstern, E.H. *Turbulent Flow Pressure Drop Model for Fuel Rod Assemblies Utilizing a Helical Wire-Wrap Spacer System* / E.H. Novendstern // Nuclear Engineering and Design. 1972. V. 22, pp. 19-27.